STRUCTURE CHARACTERIZATION AND CORROSION BEHAVIOR OF Zn-Al-Mg ALLOY WITH ADDITION OF TIN

KUSÝ Martin, GONDEK Ján, BABINEC Martin

Slovak University of Technology, Faculty of Materials Science and Technology, Institute of Materials Science, Trnava, Slovakia, EU

Abstract

Zn and Zn-based alloys attract interest due to an ability to protect steel surface against corrosion. Thin surface layer of a protective zinc alloy is usually prepared by hot dip galvanizing and acts as a barrier against corrosive environment or as a sacrificial anode in case the bare steel surface is exposed. Ability of zinc to protect steel surface against corrosion can be further increased by addition of alloying elements such as for example Al and Mg. These could be added in different amounts leading to a several-fold increase in corrosion resistance. Further elements are therefore studied in order to understand their effect on corrosion behavior and other properties such as for example ductility, hardness, wear resistance, etc.

The aim of this paper is characterization of the ternary alloy Zn - 1.6 wt.% Al - 1.6 wt.% Mg which is further modified with addition of tin in a range from 0 up to 3 wt.%. Prepared by melting of elements with 4N purity under a Zincogen 318 flux layer in a ceramic crucible all compositions were left to solidify by air cooling outside a melting furnace. Structure analysis of as-cast alloys was carried out with a help of light microscopy (LM), scanning electron microscopy (SEM), x-ray diffraction (XRD) and differential scanning calorimetry (DSC) and led to the identification of following phases: Zn rich solid solution, Al rich solid solution, Zn_2Mg and Mg_2Sn. Furthermore, XRD was used to identify corrosion products which were formed during exposure of alloys in a salt spray chamber.

Keywords: Zn-based alloy, corrosion, salt spray test

1. INTRODUCTION

The application of steel construction materials is largely connected to the use of protective metallic coatings containing zinc [1]. The steel is protected by the Zn coating through a barrier effect and a galvanic effect, in which Zn acts as the sacrificial anode while steel acts as the cathode [2]. Various Zn alloy coating systems have been developed and some of them are applied commercially [3]. Very soon Zn-Al coatings with higher aluminum contents than the alloy used in the conventional galvanizing process, such as Galfan (Zn - 5 wt.% Al) and Galvalume (Zn - 55 wt.% Al - 1.6 wt.% Si) were developed. These coatings offer higher corrosion resistance than conventionally galvanized steel because they have the sacrificial protection of zinc and a long lasting physical barrier by forming aluminum oxide in most natural environments [4]. Besides aluminum, magnesium was found to have a positive effect on the corrosion resistance of steel coatings as well [4]. First trials to improve corrosion stability of zinc coatings with magnesium date back to the 1960s. Commercial products such as Zn - 11 wt.% Al - 3 wt.% Mg - 0.2 wt.% Si and Zn - 6 wt.% Al - 3 wt.% Mg for heavy corrosive environments have been available from the end of 1990s [2]. Mg alloying results in the formation of intermetallic phases with Zn, usually Zn_2Mg. Zn-Mg intermetallics are more active in the galvanic series than pure Zn, causing preferential corrosion [4].

Zinc coatings containing Mg and Al for corrosion protection of steel were first developed in the late 1990s. ZnMgAl (ZM) coatings have undergone extensive development over the past decade. The main objective of the efforts is to extend the service life of the coated steel by modifying the Zn-coating method without decreasing the sacrificial anodic effect [2]. Compared with conventional hot dip galvanized steel, ZM coated steel has demonstrated significantly higher corrosion resistance in accelerated corrosion tests with high

chloride content [5]. The Zn coatings alloyed with magnesium and aluminum consist of complex microstructures including Zn, Zn-Zn_2Mg binary eutectic structure and Zn-Zn_2Mg-Al ternary eutectic structure [6]. These were mainly produced as relatively thick coatings which showed improved corrosion performance for heavy corrosive building applications [3]. According to some researches binary and ternary eutectics corrode preferentially compared to Zn dendrites [7, 8].

The Zn-Sn alloy coating has good corrosion resistance and ductility [9]. The corrosion resistance of the Zn-Sn alloy strongly depends on its composition and the corrosion medium. Although the corrosion resistance of the Zn-Sn alloy is not actually lower than that of pure Zn, Sn or Cd is often used as an alternative for these metals from various practical and economic considerations [10].

Usually, Zn_2Mg phase reduces toughness of the coating [11]. As a consequence, reduction of Zn_2Mg phase amount in the structure can improve mechanical properties of the coating. An addition of Sn into coating causes formation of Mg_2Sn phase at the expense of Zn_2Mg benefiting from the fact that Mg_2Sn phase is tougher than Zn_2Mg phase. Moreover, an addition of Sn results in more stable microstructure and better mechanical properties [12].

2. EXPERIMENTAL

Corresponding amount of elements of 4N purity were melted in a ceramic crucible using furnace LAC LMV5/12 at temperature of 480 °C. After approximately 1 hour of homogenization all ingots were allowed to solidify by still air outside the furnace. Subsequently, ingots were turned by lathe and cut into discs with dimensions ϕ 30x8 mm. Chemical compositions of ingots were verified using optical emission spectrometer Spectruma GDA 750 and results are listed in **Table 1**.

Table 1 Chemical composition of as-cast ingots (wt.%)

Alloy	Zn	Al	Mg	Sn
Zn - 1.6 Al - 1.6 Mg - 0.5 Sn	Bal.	1.97	1.94	0.51
Zn - 1.6 Al - 1.6 Mg - 1 Sn		2.01	1.98	1.05
Zn - 1.6 Al - 1.6 Mg - 2 Sn		1.98	2.21	2.71
Zn - 1.6 Al - 1.6 Mg - 3 Sn		2.03	2.08	2.98

Metallographic preparation was executed in 3 consecutive steps. Grinding using SiC papers from grit 240 to 4000, polishing from 3 µm to ¼ µm using water free diamond slurries and etching with 0.3 % Nital were applied.

In order to characterize sequence of transformations during solidification and cooling from molten state a DSC experiments were suggested. After cutting thin pieces from an ingot, a small, max. 5 mg sample was prepared, weighted using precision laboratory balance Mettler Toledo XP204 and placed in graphite crucible. Melting temperature and temperatures of phase transformations were observed using power compensated Perkin Elmer Diamond DSC. Sample was heated up to 480 °C and cooled down with rate of 10 K/min with short equilibrating step at 480 °C with dwell time of 10 minutes.

Microstructure was characterized using light microscope Zeiss AxioImager.Z2m and SEM Jeol JSM 7600F with FEG cathode. Back scattered electrons BSE collected with Retractable Backscattered Electrons Imaging (RBEI) detector were used to compose images of microstructure in z-contrast. Information about local chemical composition was collected using EDX analyzer Oxford Instruments X-Max 50 mm^2. Observations were performed using 15 kV accelerating voltage, 89 µA beam current. Samples were maintained at constant working distance WD of 15 mm.

XRD experiments have been performed using PANalytical Empyrean diffractometer with Bragg-Brentano geometry and iron filtered CoKα characteristic radiation. Measurements were executed at room temperature

and with sample spinning. The patterns were recorded over a two-theta range 30-110°. For more precise characterization of phases on the corroded surface a grazing incident GI XRD experiment at a constant ω angle of sample 2, 4 and 6° were executed in the range from 5 to 120°. GI experiment utilized X-ray parallel beam optics on primary beam and scintillation detector on a diffracted beam side.

As-cast ingots cut into discs were covered by protective layer of Lacomit varnish and only one side was exposed to a corrosion environment in a corrosion chamber. Corrosion environment was made by 5% water solution of analytical grade NaCl and the corrosion chamber made by CO.FO.ME.GRA type 400LE (total internal volume 400 l) was used. After 250 h of exposure time, samples were cleaned in 10% water solution of CrO_3 assisted with ultrasonic cleaner. Corroded surface was immersed in CrO_3 and their weights were measured several times till the weight reproduced. Samples weights were measured before and after salt spray test using laboratory scale Mettler Toledo XP204.

3. RESULTS

Microstructure of as-cast samples was examined using SEM which has revealed typical solidification microstructures formed in the center of the ingot. Images representing solidification microstructure containing primary dendrites, monotectoid, binary, ternary and quaternary eutectic are shown in **Fig. 1**. Chemical composition of individual phases was determined using EDX. At least three distinct clusters of chemical compositions were recognized, Zn rich solid solution with minor amount of Al, Zn and Mg rich phase with Zn:Mg ratio 2:1, Mg and Sn rich phase with Mg:Sn ratio equal 2:1 and finally Zn and Al rich phase.

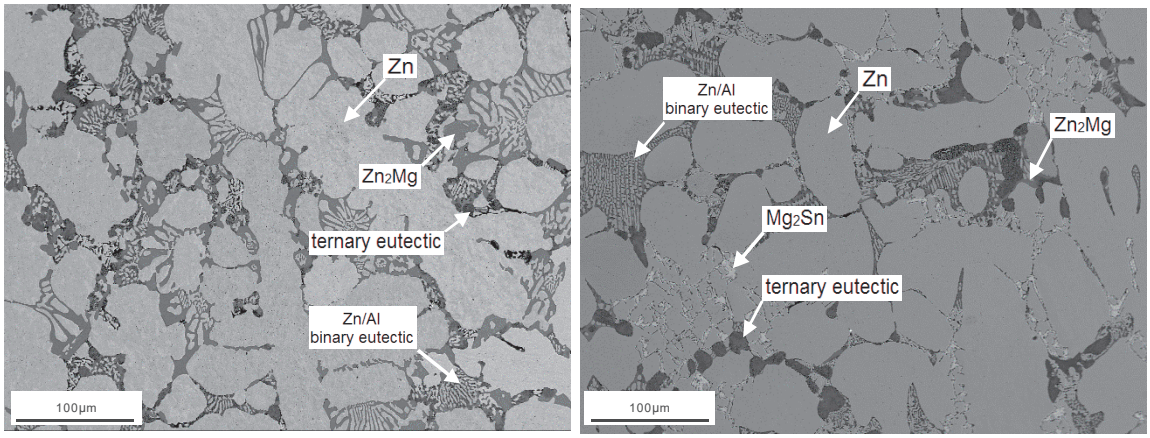

Fig. 1 As-cast microstructure of the Zn-Al-Mg-Sn ingots: Zn - 1.6 Al - 1.6 Mg - 0.5 Sn and Zn - 1.6 Al - 1.6 Mg - 3.0 Sn images with z-contrast

XRD patterns of Zn - 1.6 Al - 1.6 Mg - 0.5 Sn and Zn - 1.6 Al - 1.6 Mg - 2 Sn are exemplified in **Fig. 2**. In both cases, alloys contain Zn-based solid solution, Zn_2Mg and Al solid solution. Alloy containing 2 wt.% of Sn contains also Mg_2Sn intermetallic phase.

As-cast microstructure evolves upon cooling during solidification. DSC experiment revealed that studied alloys transformed from liquid into solid state in a series of transformations. Reactions are recorded during DSC measurement as individual well resolved or overlapping endothermic peaks. Complexity of crystallization process appears to decrease with increasing Sn amount. In case of all alloys, however, beginning of solidification takes place by crystallizing Zn-rich solid solution at around 360 °C. Further crystallization events were observed at around 340 °C and 330 °C corresponding to the formation of a binary eutectic: Zn solid solution - Zn_2Mg and ternary eutectic Zn-solid solution - Zn_2Mg - Al solid solution.

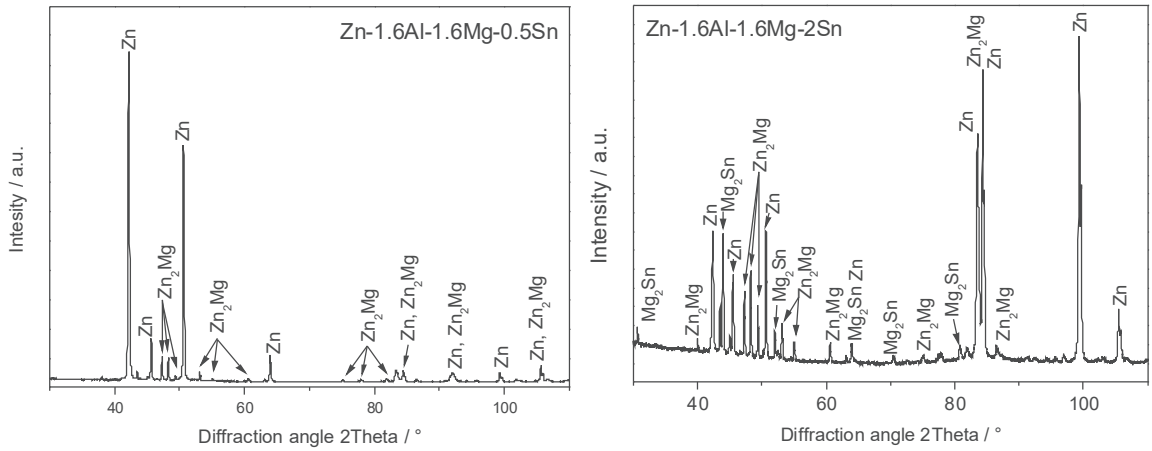

Fig. 2 XRD patterns of Zn - 1.6 Al - 1.6 Mg - 0.5 Sn and Zn - 1.6 Al - 1.6 Mg - 2 Sn with corresponding phases

As-cast samples were exposed to a corrosion environment in a salt spray chamber for a period of 250 and 500 hours. Evolved corrosion products were analyzed using XRD in grazing incidence mode. Samples cleaned from corrosion products were subsequently measured for actual weight after the salt spray test. Summary of results is shown in **Table 2** and documents that samples of all experimental alloys gained weight despite thorough surface cleaning which locally regained former luster after polishing. This is documented in **Fig. 3a** in case of sample Zn - 1.6 Al - 1.6 Mg - 3 Sn. Removal of corrosion products from the surface of this particular sample revealed formation of macroscopic blisters. Height of blisters was evaluated using laser scanning confocal microscopy with profile analysis to reach approximately 40 μm, as it is shown in **Fig. 3b**.

Table 2 Sample weight after salt spray test and corrosion product removal

Sample	Weight before (g)	Weight after (g)	Difference (g)
Zn - 1.6 Al - 1.6 Mg - 0.5 Sn	40.8488	40.8525	+0.0037
Zn - 1.6 Al - 1.6 Mg - 1 Sn	31.6275	31.6307	+0.0032
Zn - 1.6 Al - 1.6 Mg - 2 Sn	33.2946	33.2995	+0.0049
Zn - 1.6 Al - 1.6 Mg - 3 Sn	32.2053	32.2352	+0.0299

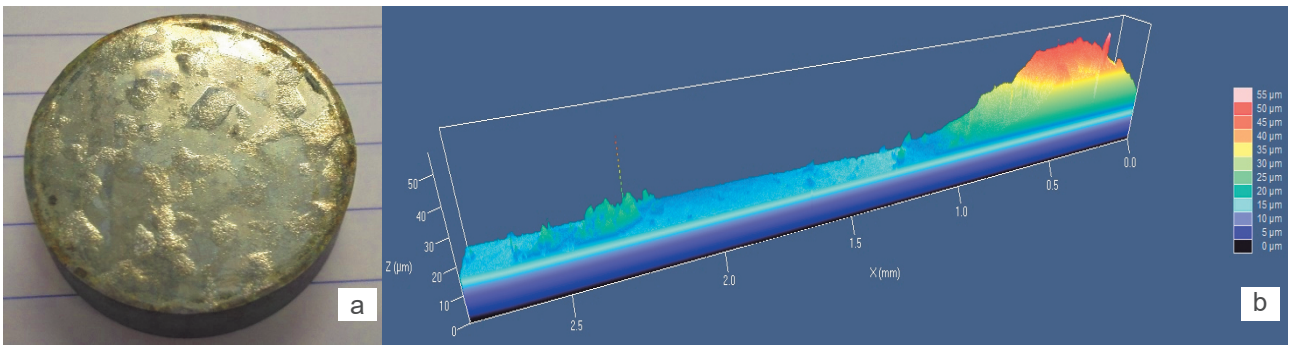

Fig. 3 Macroscopic appearance of Zn - 1.6 Al - 1.6 Mg - 3.0 Sn

According to GI XRD analysis of Zn - 1.6 Al - 1.6 Mg - 2 Sn alloy (**Fig. 4**), corrosion products formed during salt spray test consists of phases typical for as-cast state accompanied with simonkolleite, hydrotalcite after 250 hours and in addition also with hydrozincite after 500 hours of exposition.

Metallographic cross-section is shown in **Fig. 5** and it provides insight into the blister formation. Cracks containing higher concentration of Cl and O are developed at the expense of eutectic regions localized in interdendritic spaces.

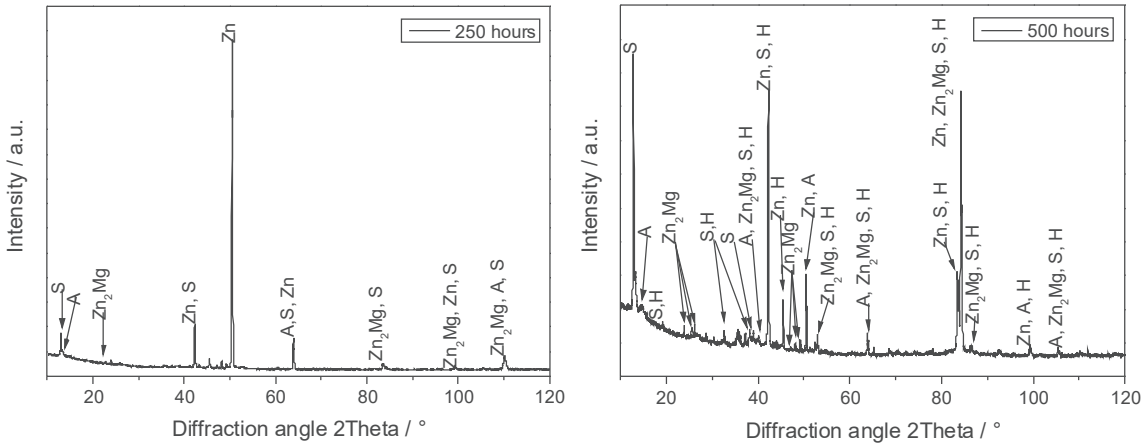

Fig. 4 GI XRD analysis of Zn - 1.6 Al - 1.6 Mg - 2 Sn after salt spray test in a period of 250 and 500 hours, where S holds for simonkolleite $Zn_5(OH)_8Cl_2.(H_2O)$, A for hydrotalcite $Mg_6Al_2(CO)_3(OH)_{16}.4(H_2O)$ and H for hydrozincite $Zn_5(CO_3)_2(OH)_6$

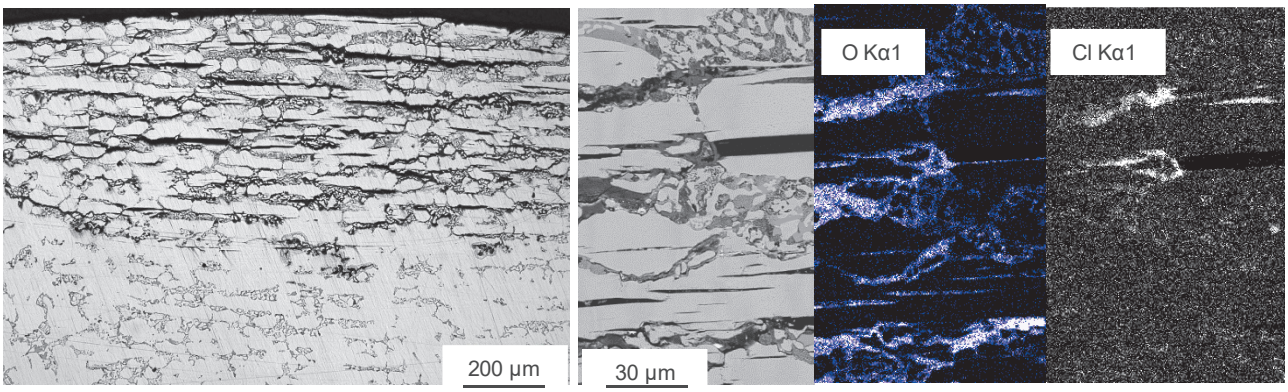

Fig. 5 Cross-section of a blister formed on the surface of an alloy containing Zn - 1.6 Al - 1.6 Mg - 2 Sn. SEM z-contrast image and corresponding O and Cl element map.

4. DISCUSSION AND CONCLUSIONS

Ternary alloys Zn - 1.6 Al - 1.6 Mg were modified by addition of tin in the following range: 0, 0.5, 1.0, 2.0 and 3.0 wt.% Sn to study effect of the corrosion resistance in Cl containing environment. As-cast samples were cooled slowly by still air. Initial microstructure after the solidification inspected with LM, SEM, XRD and DSC contained primary dendrites of Zn-rich solid solution surrounded with intermetallic phases Zn_2Mg and Mg_2Sn formed during binary, ternary and quaternary eutectic reactions (**Fig. 1** and **Fig. 2**). Structural component consisting of fine lamellae of Al-rich and Zn-rich solid solutions was observed as a product of monotectoid reaction. According to SEM micrographs as well as XRD the increasing addition of Sn led to a formation of Mg_2Sn which is according to [12] more favorable with respect to future mechanical properties and ductility of alloys. Exposure to Cl containing neutral environment during salt spray test was executed in range from 250 to 500 hours. XRD analyses of exposed samples (**Fig. 4**) proved formation of typical corrosion products such simonkolleite, hydrotalcite after 250 hours and in addition also hydrozincite after 500 hours, respectively. Typical weight loss determined on samples cleaned from corrosion products has not been observed. Instead, a gradual gain of weight was documented in **Table 2**. The higher was Sn content in the sample the higher was

the weight gain after the corrosion test. Sample surface cleaned from corrosion production (**Fig. 3**) revealed also presence of blisters, which were particularly pronounced in case of 3 wt.% addition tin. Metallographic cross-section of the blister studied by LM and SEM combined with oxygen and chloride element mapping (**Fig. 5**) revealed extensive formation of corrosion products at the expense of phases located in interdendritic spaces which corroborate well with results available in [13]. Formation of blisters especially in case of higher tin amounts significantly deteriorates corrosion resistance of alloys. It also suggests that replacement of Zn_2Mg with more favorable Mg_2Sn is limited. Further study of effects of Sn addition on mechanical properties is however required in order to understand its complete role.

ACKNOWLEDGEMENTS

Authors would like to acknowledge financial support provided by Slovak Scientific Grant Agency VEGA in the frame of 1/0068/14 project.

REFERENCES

[1] PROSEK T., NAZAROV A., BEXELL U., THIERRY D., SERAK J. Corrosion mechanism of model zinc-magnesium alloys in atmospheric conditions. Corrosion Science, Vol. 50, 2008, pp. 2216-2231.

[2] DILER E., ROUVELLOU B., RIOUAL S., LESCOP B., NGUYEN VIEN G., THIERRY D. Characterization of corrosion products of Zn and Zn-Mg-Al coated steel in a marine atmosphere. Corrosion Science, Vol. 87, 2014, pp. 111-117

[3] KYOO YOUNG K., BOO YOUNG Y. An electrochemical study on Zn-Sn-alloy-coated steel sheets deposited by vacuum evaporation. Surface and Coatings Technology, Vol. 64, 1994, pp. 99-110.

[4] SCHRUERZ S., FLEISCHLANDERL M., LUCKENEDER G. H., PREIS K., HAUNSCHMIED T., MORI G., KNEISSL A. C., Corrosion behaviour of Zn-Al-Mg coated steel sheet in sodium chloride-containing environment, Corrosion Science, Vol. 51, 2009, pp. 2355-2363.

[5] SALGUEIRO A.M., ALLÉLY C., OGLE K., VOLOVITCH P., Corrosion mechanisms of Zn(Mg, Al) coated steel in accelerated tests and natural exposure: 1. The role of electrolyte composition in the nature of corrosion products and relative corrosion rate. Corrosion Science, Vol. 90, 2015, pp. 472-481.

[6] H.-K. SOHN, J.-W. LEE, Y. YOO, J. MIN, M.-S. OH, S.-H. KIM, Y.-S JIN, K. Y KIM. Corrosion Behaviors of Zn-$MgZn_2$ Eutectic Structure in Zn-Al-Mg Coatings, Galvatech 2011

[7] SALGUEIRO AZEVEDO M., ALLÉLY C., OGLE K., VOLOVITCH P., Corrosion mechanisms of Zn(Mg,Al) coated steel: 2. The effect of Mg and Al alloying on the formation and properties of corrosion products in different electrolytes. Corrosion Science, Vol. 90, 2015, pp. 482-490.

[8] DUTTA, M., HALDER, A.K., SINGH, S.B. Morphology and properties of hot dip Zn-Mg and Zn-Mg-Al alloy coatings on steel sheet. Surf. Coat. Technol., Vol. 205, 2010, pp. 2578-2584.

[9] KYOO YOUNG K., BOO YOUNG Y. An electrochemical study on Zn-Sn-alloy-coated steel sheets deposited by vacuum evaporation. Part I: Surface and Technology, Vol. 64, Issue 2, May 1994, pp. 99-110.

[10] SZIRÁKY L., CZIRÁKY A., VÉRTESY Z., KISS L., IVANOVA V., RAICHEVSKI G., VITKOVA S., MARINOVA T. Zn and Zn-Sn alloy coatings with and without chromate layers. Part I: Corrosion resistance and structural analysis. Journal of Applied Electrochemistry, Vol. 29, 1999, pp. 927-937.

[11] DE BRUYCKER E., ZERMOUT Z., DE COOKMAN C.B. Zn-Al-Mg Coatings: Thermodynamic Analysis and Microstructure Related Properties. Materials Science Forum, Vols. 539-543, 2007, pp. 1276-1281.

[12] GHOSH P., MEZBAHUL-ISLAM M., MEDRAJ M. Critical assessment and thermodynamic modeling of Mg-Zn, Mg-Sn, Sn-Zn and Mg-Sn-Zn systems. CALPHAD: Computer Coupling of Phase Diagrams and Thermochemistry, Vol. 36, 2012, pp. 28-43.

[13] KWEON Y.G., CODDET C. Behavior in seawater of zinc-base coatings on aluminum alloy 5086. Corrosion, Vol. 48, No. 2, 1992, pp. 97-102.